A Planar Rectenna at 2.45 GHz With Circular Polarization for Wireless Power Transmission

Ayoub Elmai[1*], *Jamal* Zbitou[1,2], *Noha* Chahboun[1], *Stéphane* Ginestar[3], and *Mohammed* El Gibari[3]

[1]LABTIC, ENSA of Tangier, Abdelmalek Essaâdi University, Tetouan, Morocco
[2]LABTIC, ENSA of Tetouan, Abdelmalek Essaâdi University, Tetouan, Morocco
[3]Nantes Université, CNRS, IETR, UMR 6164, F-44000 Nantes, France

Abstract. This study presents the design and analysis of a compact circularly polarized rectenna operating at 2.45 GHz, intended for wireless power transmission (WPT) applications. The proposed structure includes a 2x2 patch array antenna and a voltage doubler rectifier circuit, both optimized to maximize RF-DC conversion efficiency. Simulations, carried out using ADS and another electromagnetic solver show excellent performance with a reflection coefficient (S_{11}) below -10 dB, an axial ratio below 3 dB in the ISM band, and a maximum gain of 11.14 dB for the antenna array. The RT5880 substrate (ε_r = 2.2, tanδ = 0.0009) and 35 µm metal thickness were chosen to balance performance and simplicity of design. The results show an RF-DC conversion efficiency of up to 73.69% at 27 dBm, confirming the potential of this design for mobile WPT applications such as powering drones.

1 Introduction

Wireless power transfer (WPT) has emerged as a promising technology that challenges traditional wired power delivery methods, drawing growing interest across various applications [1–3]. Among the key enabling components of WPT systems is the rectenna, which plays a critical role in converting captured RF energy into usable DC power for powering low-energy electronic devices [4–6]. With the increasing demand for mobility, compactness, and energy autonomy especially in applications such as Internet of Things (IoT) devices and drones WPT systems must be designed with a focus on size reduction, cost-effectiveness, and integration efficiency [7].

A rectenna system generally consists of three essential components: an antenna to capture the RF signal, a matching network to optimize power transfer, and a rectifying circuit to convert RF to DC power. The antenna design largely determines the system's overall size and integration complexity. For example, probe-fed microstrip patch antennas often lead to multilayer structures, where the antenna and rectifier are placed on different layers while sharing a common ground plane. This approach helps minimize electromagnetic interference between the antenna and the rectifier [8].

* Corresponding author: ayoub.elmai@etu.uae.ac.ma

In this regard, circular polarization (CP) offers a significant advantage [9–11]. Unlike linearly polarized antennas, CP antennas are less sensitive to orientation mismatch between the transmitter and receiver, making them highly suitable for mobile or dynamically positioned targets [12–14]. Additionally, CP antennas perform more reliably under varying propagation conditions such as scattering or multipath, which are common in real-world environments.

This work proposes the design and simulation of a compact planar rectenna operating at 2.45 GHz. The system consists of a circularly polarized 2×2 patch antenna array integrated with a voltage doubler rectifier using two Schottky diodes. The objective is to achieve high gain, improved RF-to-DC conversion efficiency, and robust performance regardless of the angle of incidence of the incoming wave thus meeting the critical demands of mobile wireless power transfer, including applications such as drones. Section 2 covers the theoretical background of rectennas and rectifiers, Section 3 discusses the design, simulation, and implementation, and Section 4 provides conclusions and Future work.

2 Rectenna theory

As depicted in Figure 1, a fundamental rectenna structure integrates a low-pass filter (LPF) positioned between the antenna and the rectifying circuit. This LPF is crucial for allowing the fundamental frequency to pass while reflecting a significant portion of the higher-order harmonics generated by the non-linear rectification process back towards the rectifying circuit. This circuit typically employs a single diode in a shunt configuration across the transmission lines. The microwave power conversion within this rectifying stage operates similarly to a diode clamping circuit or a large-signal mixer at microwave frequencies. Optimal power conversion efficiency is achieved by confining these higher-order harmonics between the low-pass filter and the DC pass filter, utilizing an efficient diode, and ensuring proper impedance matching between the diode's input and the antenna [15].

A diode's power conversion efficiency is inherently dependent on the operating power level, which consequently influences the rectenna's overall efficiency as illustrated in Figure 2. In this figure, V_j, V_{br}, and R_L respectively denote the diode's forward voltage drop (junction voltage), breakdown voltage, and the rectenna's DC load resistance. At low input power levels, efficiency remains modest because the voltage swing across the diode is insufficient, being less than or comparable to its forward voltage drop. As the input power increases, the efficiency improves until it eventually plateaus, primarily due to the generation of strong higher-order harmonics [15].

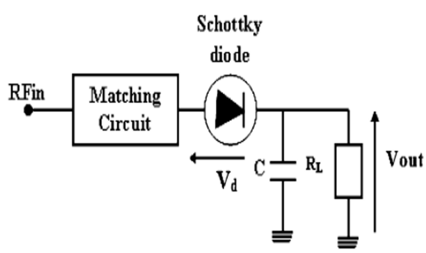

Fig. 1. Series microwave rectifier configuration [16].

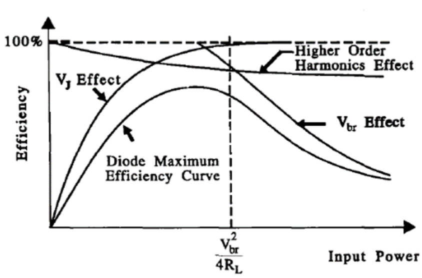

Fig. 2. General relationship between microwave to dc power conversion efficiency and input power.

The efficiency of the microwave rectifier is expressed as :

$$\eta = \frac{P_{DC}}{P_{LOSS} + P_{DC}} \tag{1}$$

The following terms are defined as: load resistance (R_L), $P_{DC} = \frac{{V_{out}}^2}{R_L}$ (DC output power across the load (R_L)), and power losses (P_{LOSS}). In a simplified model where, other losses are considered negligible, the primary factor limiting conversion efficiency is the diode's conduction losses. This simplified efficiency can be approximated using the methodologies described in [17] and [18].

$$\eta = \frac{1}{1 + \frac{V_d}{2V_{out}}} \tag{2}$$

The voltage drop across the conducting diode is represented by the relevant parameter V_d . As illustrated in Figure 2, the simulated RF-to-DC conversion efficiency demonstrates an increase with input power beyond a threshold of 20 dBm. This efficiency reaches its peak at 68% when the input power is 20 dBm. The DC equivalent circuit for a Schottky barrier diode (SBD) comprises a voltage source connected in series with its junction resistance R_j[19]. Consequently, the rectifier's output voltage can be formulated as:

$$V_{out} = V_{DC} \frac{R_L}{R_L + R_j} \tag{3}$$

We define V_{DC} as the DC component of the diode junction voltage and R_j as the junction resistance of the Schottky diode. R_j is obtained by differentiating the diode's voltage-current characteristic, as shown in [20].

$$R_j = \frac{nKT}{q(I_s + I_b)} \tag{4}$$

The conversion efficiency (η) of the rectenna can be calculated using the following formula:

$$\eta(\%) = \frac{V_L^2}{R_L\, P_r} \times 100\% \tag{5}$$

Where V_L is the output voltage across the load, R_L is the load resistance, and P_r represents the power received by the antenna. The received power P_r can be determined by the Friis transmission equation as:

$$P_r = (\frac{\lambda}{4\pi r})^2 G_t G_r P_t \tag{6}$$

In this equation, λ denotes the wavelength at the operating frequency, G_t and G_r are the gains of the transmitting and receiving antennas respectively, $P_t$is the transmitted power, and *r* is the distance separating the transmitting antenna and the rectenna [21].

3 Design and Simulation Results

3.1 Design a Microstrip RF-DC Rectifier

The circuit shown operates as a voltage doubler rectifier (VDR), designed to increase the amplitude of incoming RF signals. It uses HSMS-2820 Schottky diodes, chosen for their low forward voltage (340 mV), which ensures fast switching and high efficiency. The rectifier consists of two main parts: a peak detector formed by D1 and C1, and a voltage clamp using D2 and C2 [15].

For impedance matching, microstrip transmission lines are used TL4 at the input and TL5 at the output optimized to reduce signal loss and improve RF-to-DC conversion. The design is implemented on an FR4 substrate (ε_r= 4.4, thickness = 1.6 mm), resulting in a compact and efficient layout suitable for space-limited systems like rectennas and antenna arrays [15].

An output filter, made of a capacitor and a quarter-wavelength (λ/4) line, helps stabilize the DC output and recycle harmonic energy to boost conversion efficiency. The full design, including schematic, layout, and simulation, was carried out using ADS (Advanced Design System) by Agilent Technologies. Accurate diode modelling was ensured by using key parameters from the ADS library, such as series resistance (Rs = 6 Ω), junction capacitance (Cj_0 = 0.7 pF), and breakdown voltage (V_B = 15 V) [15].

Figure 3 illustrates the schematic of the voltage doubler rectifier.

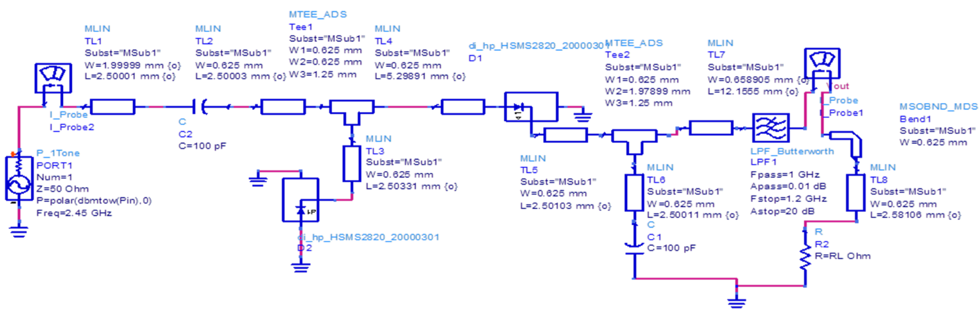

Fig. 3. The schematic of the voltage doubler rectifier [15].

As shown in Figure 4, efficiency (η) is low for input power levels below P_{in} = 0 dBm. A significant improvement is observed near $P_{in} \approx$ 10 dBm, peaking at η = 73.69% at 27 dBm, when $P_{in} <$ 10 dBm. This suggests the circuit lacks sensitivity at low input powers.

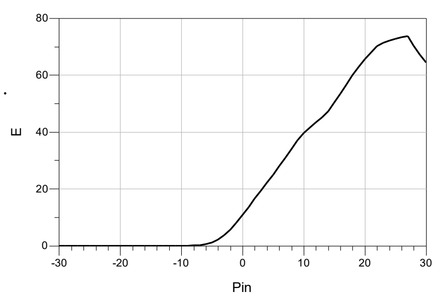

Fig. 4. RF–DC conversion efficiency versus input power rectifier using two HSMS2820 Schottky diodes [15].

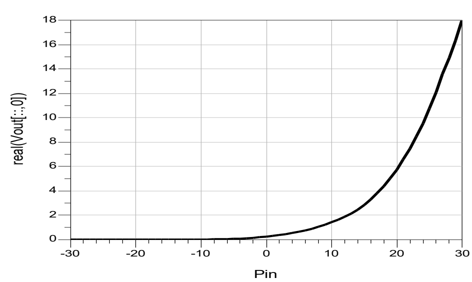

Fig. 5. Output voltage versus input power for the for the rectifier using one single HSMS2820 Schottky diode [15].

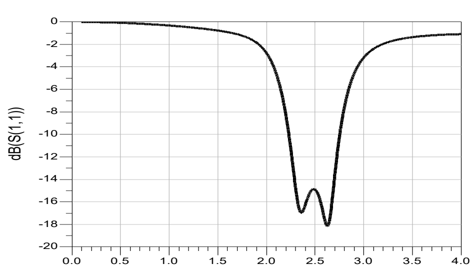

Fig.6. S11 versus input power at 2.45 GHz [15].

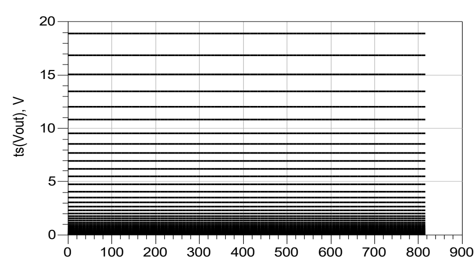

Fig. 7. Smoothed Output Voltage After Butterworth Filter Application [15].

Figure 5 illustrates the relationship between output voltage V_{out} and input power P_{in} for the rectifier employing a single HSMS2820 Schottky diode. As the input power increases, V_{out} rises progressively, with a significant improvement in performance observed starting around $P_{in} = 0$ dBm indicating that the circuit begins to operate efficiently in this range. At higher input power levels (above 25 dBm), the output voltage gradually stabilizes, reaching a maximum value of approximately 17.94 V at P_{in} of 30 dBm.

Figure 6 shows the S11 parameter as a function of input power at 2.45 GHz. A pronounced dip is observed at this frequency, with an S11 value of –15.186 dB, indicating good impedance matching. This suggests that the majority of the incident power is effectively transferred to the circuit, with minimal reflection.

To obtain a stable DC output voltage with minimal ripple, a Butterworth filter is integrated into the rectifier, as illustrated in Figure 3. This configuration effectively smooths the rectified signal (Figure 7), enhancing the quality of the DC output for subsequent use in energy harvesting applications [15].

3.2 Antenna design polarization circular

In this figure, a square microstrip patch antenna is designed to operate at 2.45 GHz using the RT/Duroid 5880 substrate, which has a relative permittivity (ε_r) of 2.2, a thickness (h) of 1.57 mm, and a low loss tangent of 0.0009. The patch has a copper thickness of 0.035 mm and is fed with a 50 Ohm line.

To achieve circular polarization, the truncated corners technique is applied. The antenna patch is initially designed as a square, where the width **W** and length **L** of the patch are approximately equal [21].

The width **W** is calculated using the following formula :

$$\mathrm{W} = \frac{\mathrm{C}}{2f_r}\sqrt{\frac{2}{\varepsilon_r+1}} \tag{7}$$

The effective dielectric constant ε_{eff} is:

$$\varepsilon_{eff} = \frac{\varepsilon_r+1}{2} + \frac{\varepsilon_r-1}{2}\left(1+\frac{12h}{W}\right)^{-1/2} \tag{8}$$

The effective length L_{eff} and the extension due to fringing ΔL are given by:

$$\Delta L = 0.412h\frac{(\varepsilon_{eff}+0.3)(\frac{W}{h}+0.264)}{(\varepsilon_{eff}-0.258)(\frac{W}{h}+0.8)} \tag{9}$$

$$L = \frac{C}{2f_r\sqrt{\varepsilon_{eff}}} - 2\Delta L \tag{10}$$

To achieve circular polarization, a square patch is truncated at two opposite corners. The optimal truncation length t is chosen to be approximately:

$$t \approx \frac{L}{10} \tag{11}$$

In this design, the truncation length is chosen as t = 3.9 mm which ensures good circular polarization. This structure is shown in the figure, where the square shape of the patch and the two cut corners are clearly visible.

 https://doi.org/10.1051/e3sconf/202568000038

The Figure 8 illustrates the layout of the microstrip patch antenna designed to achieve circular polarization when the parameters (**W=L**=39.6 mm, $\mathbf{L}_f$ =23 mm ,$\mathbf{W}_f$=1.7 mm).

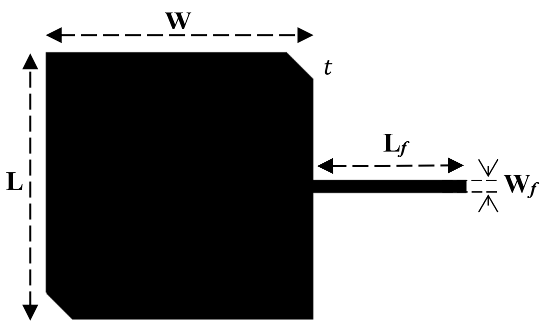

Fig.8. Layout of the microstrip patch antenna with truncated corners for circular polarization.

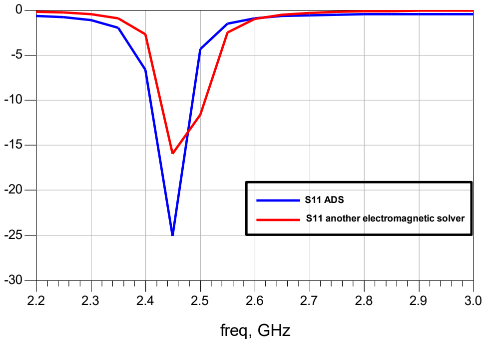

Fig.9. S11 parameter of the antenna at 2.45 GHz Using ADS & another electromagnetic solver

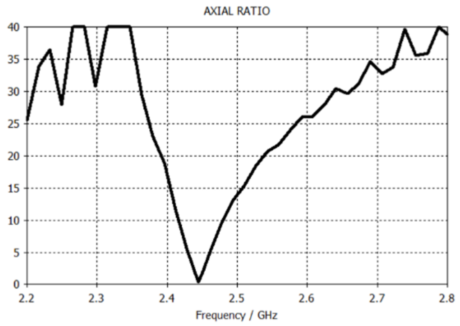

Fig.10. Axial ratio confirming circular polarization with a value below 3 dB .

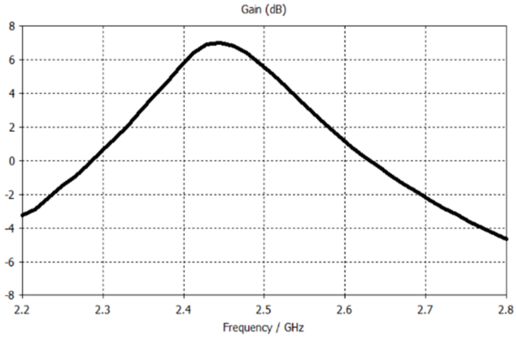

Fig.11. Gain versus frequency for a standalone patch antenna at 2.45 GHz.

By examining the results for the single patch antenna, it is immediately clear that it is well matched around 2.45 GHz (Figure 9). The reflection coefficient S11 reaches approximately -25 dB in ADS and -16 dB in another electromagnetic solver, indicating excellent impedance matching with very little power reflected at the operating frequency.

Figure 10 shows that the axial ratio is also very good, it remains below 3 dB over a bandwidth of around 100 MHz, with a minimum value close to 0.5 dB exactly at 2.45 GHz, confirming effective circular polarization.

As shown in Figure 11, the simulated gain reaches approximately 7 dB . The S11 curves obtained from ADS and another electromagnetic solver are very similar, which enhances the reliability of the results. This consistency between the two simulation tools confirms that the electromagnetic behaviour of the patch antenna is well controlled.

3.3 The design of 2x2 patch array

After designing a circularly polarized patch antenna, a 2x2 patch array antenna configuration is implemented to improve gain, directivity, and efficiency, which are important for RF energy harvesting applications.
The elements are spaced by λ/2 (61.22 mm at 2.45 GHz) to ensure phase coherence and reduce mutual coupling. Each patch maintains the same structure as the single antenna.
A microstrip power divider of the corporate feed type is used to feed the four elements with equal amplitude and phase, using lines matched to 50 ohms.
The characteristic impedance between sections is calculated using:

$$Z_C = \sqrt{Z_{int} \times Z_L} \tag{12}$$

This setup ensures stable circular polarization and a focused, high-efficiency radiation pattern.

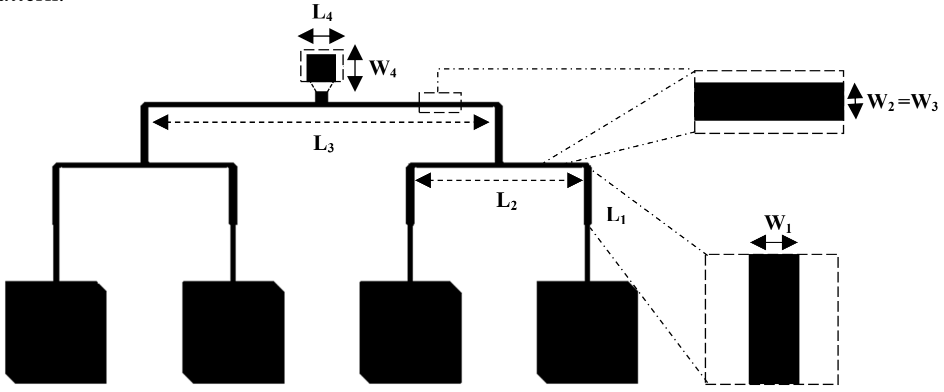

Fig.12. Layout of the 2×2 Circularly Polarized Antenna Array Design in ADS.

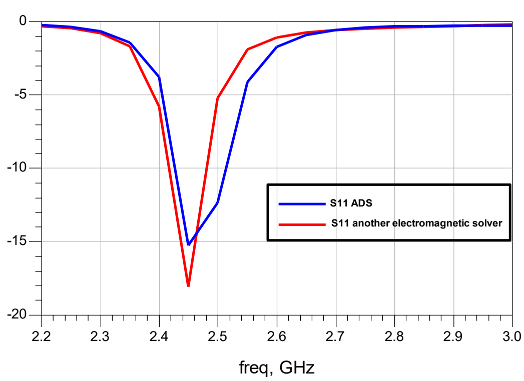

Fig.13. Simulated S11 Parameter of the 2×2 Antenna Array Using ADS & another electromagnetic solver.

Table 1. Values of the different parameters of 2x2 patch array antenna.

Parameters	Value (mm)
W_1	2.71
L_1	22.67
W_2	1.35
L_2	70
W_3	1.35
L_3	140
W_4	4.79
L_4	4.79

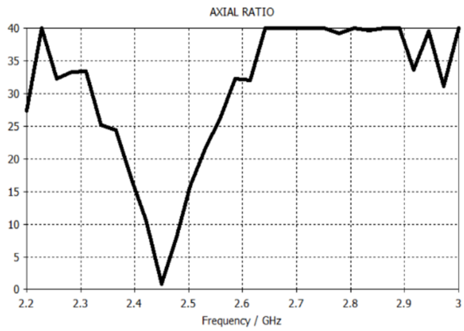

Fig.14. Axial ratio confirming circular polarization with a value below 3 dB .

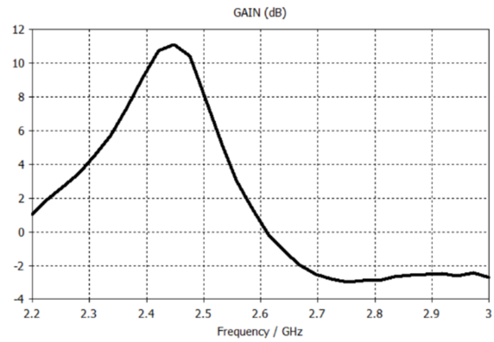

Fig.15. Gain versus frequency for the 2×2 antenna array at 2.45 GHz.

For the 2×2 antenna array, the performance is clearly improved. Figure 13 shows that the S11 remains low, reaching approximately (-18 dB) in ADS and (-15 dB) in another electromagnetic solver, still centred around 2.45 GHz. This indicates good impedance matching.
As illustrated in Figure 14, the axial ratio remains below 3 dB over a similar bandwidth, with a minimum value around 0.8 dB, indicating that circular polarization is well maintained at the array level.
According to Figure 15, the total gain increases significantly, reaching approximately 11.14 dB, which is consistent with the use of four radiating elements. Once again, the results from another electromagnetic solver and ADS are in very good agreement whether for S11, axial ratio, or gain confirming the validity of the simulated model and the overall reliability of the design.

4 Conclusion

This study presents the design and simulation of a planar rectenna operating at 2.45 GHz with circular polarization, intended for wireless power transmission (WPT) applications. The rectenna integrates a voltage-doubler rectifier circuit with a circularly polarized 2×2 microstrip patch antenna array. The design and analysis were conducted using both ADS and another electromagnetic solver simulation tools to ensure consistency and accuracy.
The antenna array demonstrates excellent impedance matching at 2.45 GHz, with a reflection coefficient (S11) reaching –18 dB in ADS and –16 dB in another electromagnetic solver, indicating minimal power reflection. Circular polarization is effectively achieved, with an axial ratio below 3 dB over a bandwidth of approximately 100 MHz, and a minimum value of 0.8 dB at the resonant frequency. The array configuration also improves radiation characteristics, with a simulated gain of around 11.14 dB in both tools, compared to 7 dB for the single patch element. The close agreement between another electromagnetic solver and ADS results strengthens confidence in the model accuracy.
Furthermore, the integrated rectifier circuit, optimized and validated through harmonic balance and co-simulation techniques, shows promising RF-to-DC conversion performance at the operating frequency. Future work will involve the fabrication of a physical prototype and experimental testing to verify the simulated performance and optimize the rectenna under real-world operating conditions.

References

1. K.M.Z. Shams, M. Ali, IEEE Sens. J. 7, 1573 (2007)
2. M. Sudou, H. Takao, K. Sawada, M. Ishida, Sens. Actuators A 145-146, 343 (2008)
3. M.A. Adeeb et al., Act. Passive Electron. Compon. 2012, 879294 (2012)
4. J.-Y. Park, S.-M. Han, T. Itoh, IEEE Antennas Wirel. Propag. Lett. 3, 52 (2004)
5. T.-C. Yo et al., IEEE Trans. Antennas Propag. 56, 882 (2008)
6. L.W. Epp et al., IEEE Trans. Microw. Theory Tech. 48, 111 (2000)
7. M. Ali, G. Yang, R. Dougal, IEEE Antennas Wirel. Propag. Lett. 4, 205 (2005)
8. H.J. Visser et al., EDN 52, 34 (2007)
9. R. Jin et al., in Proc. 2014 Int. Workshop Antenna Technol. (iWAT), Sydney, Australia, 140 (2014)
10. S. Li et al., Mod. Radar 31, 75 (2005)
11. G. Yang et al., Prog. Electromagn. Res. 5, 153 (2008)
12. J. Pourahmadazar, S. Mohammadi, Electron. Lett. 45, 837 (2009)
13. J. Pourahmadazar et al., IEEE Antennas Wirel. Propag. Lett. 10, 369 (2011)
14. J.-S. Row, IEEE Trans. Antennas Propag. 53, 1967 (2005)
15. A. Elmai, J. Zbitou, Y. Laaziz, N. Chahboun, A. Tajmouati and E. Ahmed, "A New Configuration of a Microstrip RF-DC Rectifier for RF Energy Harvesting Applications," 2025 International Conference on Functional Materials and Renewable Energies (COFMER'05), EPJ Web of Conferences, vol. 326, art. no. 01002, 2025, doi: 10.1051/epjconf/202532601002.
16. J. Zbitou, M. Latrach and S. Toutain, "Hybrid rectenna and monolithic integrated zero-bias microwave rectifier," in IEEE Transactions on Microwave Theory and Techniques, vol. 54, no. 1, pp. 147-152, Jan. 2006, doi:10.1109/TMTT.2005.860509.
17. T. Yoo, K. Chang, IEEE Trans. Microw. Theory Tech. 40, 1259 (1992)
18. S. Djukic et al., IEEE Trans. Microw. Theory Tech. 47, 1457 (1999)
19. H. Eriksson, R.W. Waugh, Agilent Technol., Design Tip (2000)
20. B.L. Smith, M.-H. Carpentier, The Microwave Engineering Handbook Volume 1 (Chapman & Hall, London, 1993)
21. Y.Y. Shi, J.W. Jing, Y. Fan, L. Yang, Y. Li, M. Wang, AEU-Int. J. Electron. Commun. 95, 264 (2018)
22. C.A. Balanis, Antenna Theory: Analysis and Design (Wiley, Hoboken, 2005)